



**HAL**  
open science

## Prediction of AO corrected PSF for SPHERE / AOF NFM.

Arseniy Kuznetsov, Benoit Neichel, Sylvain Oberti, Thierry Fusco

► **To cite this version:**

Arseniy Kuznetsov, Benoit Neichel, Sylvain Oberti, Thierry Fusco. Prediction of AO corrected PSF for SPHERE / AOF NFM.. Adaptive Optics for Extremely Large Telescopes 7th Edition, ONERA, Jun 2023, Avignon, France. 10.13009/AO4ELT7-2023-106 . hal-04402888

**HAL Id: hal-04402888**

**<https://hal.science/hal-04402888v1>**

Submitted on 18 Jan 2024

**HAL** is a multi-disciplinary open access archive for the deposit and dissemination of scientific research documents, whether they are published or not. The documents may come from teaching and research institutions in France or abroad, or from public or private research centers.

L'archive ouverte pluridisciplinaire **HAL**, est destinée au dépôt et à la diffusion de documents scientifiques de niveau recherche, publiés ou non, émanant des établissements d'enseignement et de recherche français ou étrangers, des laboratoires publics ou privés.



## Prediction of AO corrected PSF for SPHERE / AOF NFM

Arseniy Kuznetsov<sup>a,b,c</sup>, Benoit Neichel<sup>b,c</sup>, Sylvain Oberti<sup>a</sup>, and Thierry Fusco<sup>b,c</sup>

<sup>a</sup>European Southern Observatory (ESO), Germany

<sup>b</sup>Laboratoire d'Astrophysique de Marseille, Aix Marseille Université, Institut National des Sciences de l'Univers, Centre National d'Études Spatiales

[Toulouse], Centre National de la Recherche Scientifique

<sup>c</sup>DOTA, ONERA, Université Paris Saclay [Palaiseau], Université Paris-Saclay, ONERA

### ABSTRACT

The prediction of Adaptive Optics (AO)-corrected PSFs offers considerable potential, with implications ranging from enhanced observational planning to the post-processing of astronomical data. The intricate nature of AO-corrected PSFs necessitated the development of advanced analytical models capable of efficiently capturing their intricate morphology. In this work, we utilize the TIPTOP[3] PSF model to predict on-axis PSFs produced by the SPHERE instrument of ESO's UT3. TIPTOP accepts integrated (reduced) telemetry as input. In theory, the physics-based analytical nature of TIPTOP should result in precise PSF predictions when using reduced telemetry as inputs to the PSF model. However, our research underscores a divergence from this expectation. By utilizing real on-sky datasets recorded on SPHERE, we demonstrate that the calibration of these analytical models is essential for improved prediction accuracy. This work introduces an approach to calibrating PSF models by conjoining them with a feed-forward Neural Network (NN). Furthermore, we present two methodologies to approach its training. Our findings reveal that the calibrated PSF model can achieve a prediction error of 13.6% on real on-sky datasets, while on simulated data, PSF prediction error can be further reduced to only 1.7%. Without calibration, the direct application of the PSF model results in errors of 34.6% for on-sky data and 14.8% for synthetic datasets.

**Keywords:** PSF reconstruction, PSF prediction, Adaptive Optics, PSF modelling, Machine Learning, Telemetry, Focal Plane PSF, PSF

### 1. INTRODUCTION

Within the Adaptive Optics (AO) community, there is a growing interest in accurately determining the morphology of focal-plane science-path Point Spread Functions (PSFs), primarily within the scope of AO-assisted observations.

---

Further author information: (Send correspondence to A.Kuznetsov)

A.Kuznetsov: E-mail: akuznets@eso.org

The knowledge of PSFs can prove useful in various applications, including more precise exposure time estimation or improved observation planning, where observations can be ranked based on the quality evaluated from predicted PSF morphology under specific environmental conditions. Additionally, PSFs can be used in the post-processing of astronomical observations. This is especially helpful when observing extended targets or crowded stellar fields where PSFs may not be directly accessible. Predicted PSFs can also be utilized to diagnose AO systems health and estimate the error budget.

Several types of PSF reconstruction (synonymously, PSF-R or PSF prediction) algorithms were proposed to address the abovementioned applications. Back in 1997, Véran et al.[5] proposed a PSF Reconstruction (PSF-R) method allowing one to estimate the “Atmosphere/AO” PSF solely based on the AO data (WFS measurements and deformable mirror shapes - also called telemetry). Applying the method for PUEO (the CFHT AO system), they demonstrated that the AO-PSF could be estimated to be better than 5% error for its FWHM. This seminal work, proposed already 20 years ago, initiated an effort in the AO community to provide astronomers with PSF models associated with their observations. However, even if the efforts have been continuously progressing (e.g., 140 papers on Astro-ph since 1997), the lack of scientific applications is a clear sign of the complexity of the whole process. Several factors can explain this situation. First, the impact of the telescope and instrument PSF, not encoded in the telemetry, plays a major role in the final PSF shape. In particular, calibrating instrumental NCPA in conditions as close as possible to the actual observations has been one of the main challenges. Then, the AO-PSF reconstruction assumes a perfectly calibrated AO system while operational constraints (temperature, gravity, local turbulence, misalignment) may modify the working point of the adaptive telescopes. This miscalibration information is not (or only partially) captured by the telemetry. Finally, the generalization of the PSF-R algorithm to multi-LGS systems remains a challenge. This brings us to the conclusion that the main limitation in PSF-R is not due to the accuracy of the model but to its actual calibration. Therefore, in this work, we propose an alternative approach where we significantly simplify the model and focus our efforts on trying to properly calibrate it with on-sky data.

PSF prediction can be approached within the framework of Fourier-based PSF models[4, 2, 1], such as TIPTOP, which we use extensively in this work. TIPTOP models PSF by leveraging statistical properties of the residual wavefront by breaking it down into multiple pupil-plane Power Spectral Density (PSD) contributors. It enables easy inclusion of various error contributors into the model, making it modular and flexible. The Fourier-based approach is compatible with all types of AO systems, including Laser Tomography Adaptive Optics (LTAO) and Multi-Conjugate Adaptive Optics (MCAO), which is pivotal within the context of the upcoming ELT instruments. The statistical nature of TIPTOP enables the generation of infinite-exposure PSFs in one shot without the need for extensive end-to-end simulations, making it fast and efficient. TIPTOP relies on integrated telemetry instead of full AO telemetry recorded at the loop frequency. It is beneficial since using the latter for PSF-R poses a challenge for many current and upcoming systems due to the large amount of telemetry data that needs to be stored and transferred in this case. For example, the Extremely Large Telescope (ELT) will only accommodate the storage/transfer capacity of 40TB of data per night, including science images, calibrations, and potentially some AO telemetry. This is approximately a factor 2 lower than the typical amount of data produced by a multi-WFS system (e.g., LTAO or MCAO) during a single night. Consequently, there is a pressing need to compress the volume of telemetry data used for PSF-R applications, which can be approached by utilizing Fourier-based methods and storing a reduced set of telemetry only.

It is important to note that the telemetry reduction process is also very system-specific. The PSF model also must be tailored to each AO system individually. It is valid for other PSF-R methods, as well as for TIPTOP. In this study, we focus primarily on the SPHERE instrument of UT3. It has the most extensive PSF dataset produced on VLT, with over 1300 samples available, including 360 in H-band. Moreover, SPHERE is a SCAO system, making it a more straightforward instrument to model. SPHERE can be viewed as a path-finder for future work with GALACSI Narrow-Filed Mode (NFM) and ELT instruments. As a PSF model, we employ the TipTorch code\*, which is an alternative implementation of the P3 library (part of the TIPTOP† framework).

---

\*<https://github.com/EjjeSynho/TipTorch>

†<https://github.com/astro-tiptop/TIPTOP>

## 2. DIRECT PSF PREDICTION

The main aim of this study is to achieve PSF prediction accuracy below 10%. We are not discussing this requirement here and how it would link to science cases, but we arbitrarily take it as the first reasonable goal. Also, this study will rely on the full PSF morphology and not only the SR of the FWHM: we will consider the full PSF profile to be estimated to be better than 10%.

As described above, we employ the reduced telemetry as input into the TipTorch model to predict PSFs under specified conditions. This methodology of utilizing telemetry as a direct input of the model will later be termed *direct prediction*. It is crucial to clarify the distinction between *full telemetry* and *reduced telemetry* mentioned before. In this context, full telemetry includes DM commands, slopes, site monitoring data, WFS images, raw scientific images, instrument configurations, and more. Meanwhile, the reduced telemetry is derived from the raw telemetry and includes such integrated parameters as atmospheric profiles,  $r_0$ , wind speed/direction, instrument settings, processed scientific images, etc.

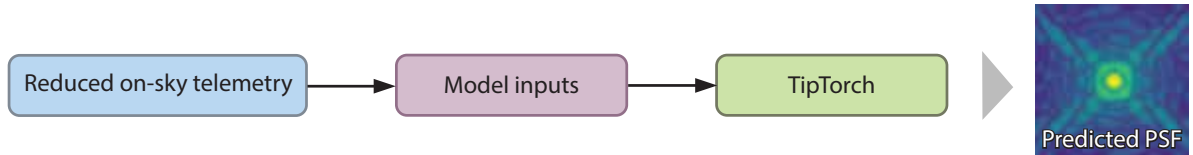


Figure 1. TIPTOP provides a full-analytical prediction of the PSF morphology based on the reduced telemetry input.

We tested the direct prediction approach on a real on-sky 360 H-band SPHERE PSFs dataset. Each data point in this dataset consists of a PSF with associated synchronously recorded reduced telemetry, making it possible to compare the model with real on-sky data. For consistency, we utilized PSFs at a single wavelength of 1.625 microns in these tests. The results are presented in Fig. 2. The radial profiles in this figure are normalized to the maximum value of a median on-sky PSF profile. The same normalization is applied for all similar figures onwards. The radial profiles are computed by averaging the radial slices of PSF with the centre at PSF intensity maximum.

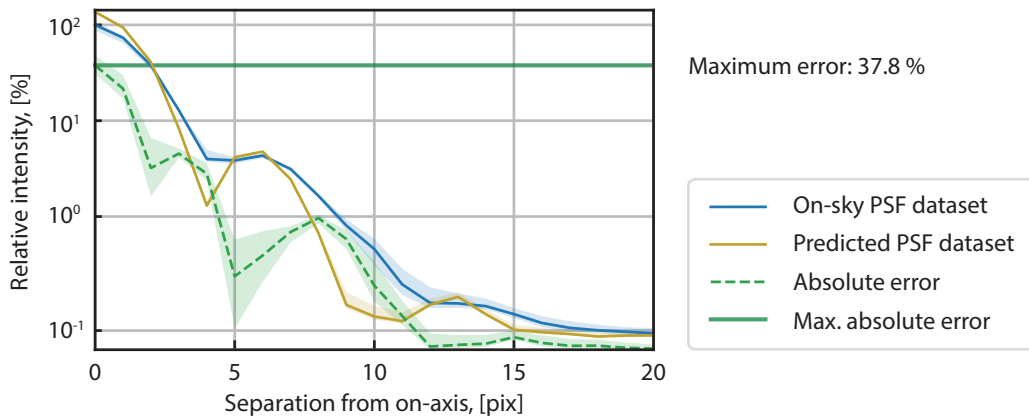


Figure 2. The prediction proved to be inaccurate when reduced telemetry is directly input into the TipTorch PSF model. This can be caused by inaccuracies and biases present in on-sky telemetry, or by potential inaccuracies in the PSF model itself.

Fig. 2 shows that direct PSF prediction proved to have very poor accuracy, way below the requirements (i.e., above 10% error). This can be attributed to two potential factors: the incomplete PSF model and/or the inaccurate telemetry inputs. Therefore, in this case, it is instrumental to first validate the PSF model. By validation, we mean proving that our model is able to fit on-sky PSFs with high accuracy.

### 3. MODEL VALIDATION

To validate the model, the approach is to fit the PSF model to the dataset of on-sky PSFs and identify the highest accuracy of the fitting achieved. The H-band dataset mentioned in the previous section was used for this purpose. The TipTorch model was fitted to each PSF in the dataset, utilizing the on-sky telemetry as an initial guess for the optimizer. The comparison between the fitted and the on-sky profiles is depicted in Fig. 3. The same fitting process was repeated for the MUSE Narrow Field Mode (NFM) PSFs, as shown in Fig. 4.

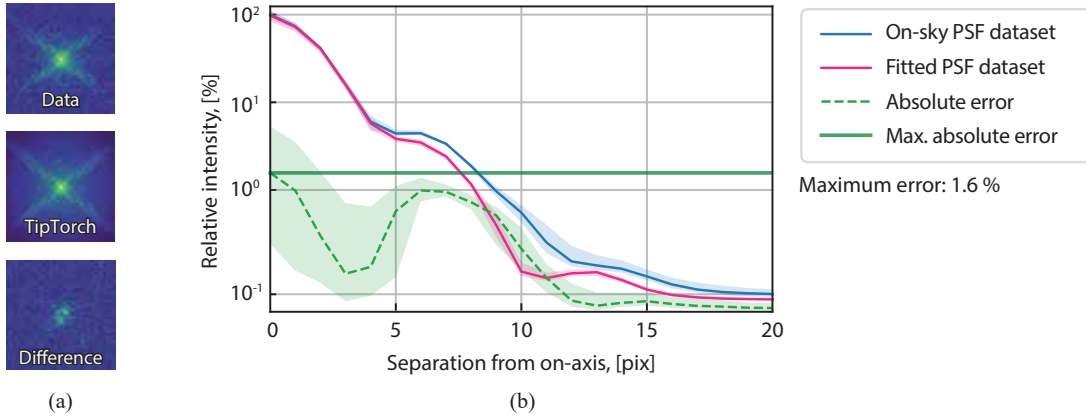


Figure 3. (a) From top to bottom (logarithmic scale): an example of on-sky SPHERE PSF, a PSF fitted with TipTorch, and the difference between on-sky and fitted PSFs. (b) The profiles of fitted SPHERE PSFs show precise correspondence to on-sky data, proving the ability of TipTop to accurately represent PSF morphology when provided with the correct inputs, which in this case are determined by fitting. Reduced telemetry here serves as an initial guess for the fitted parameters.

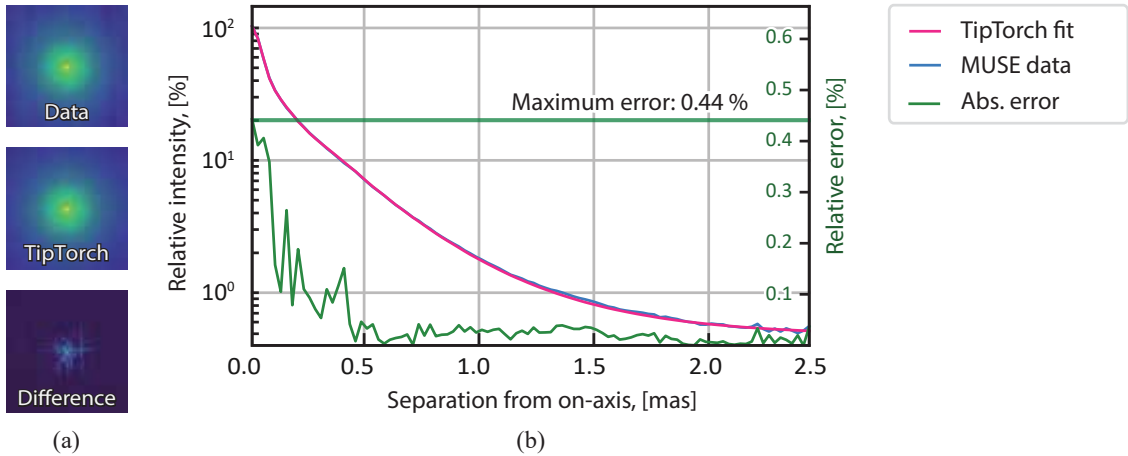


Figure 4. (a) From top to bottom (logarithmic scale): an example of on-sky MUSE NFM PSF, a PSF fitted with TipTorch, and the difference between on-sky and fitted PSFs (logarithmic scale). (b) Profiles for the same PSF.

These findings indicate that the model can accurately represent the morphology of PSFs, but only when precise inputs are utilized. Therefore, the poor accuracy of prediction described earlier can be potentially attributed to inaccuracies and biases inherent to the model inputs (and not the model itself). To enhance accuracy, we will delve into the process of calibrating the model inputs in the next section.

## 4. MODEL CALIBRATION

We propose adding a corrective transformation preceding the PSF model to implement the model calibration. This transformation acts as an intermediary between the PSF model inputs and the reduced telemetry, generating corrected inputs that lead to more accurate PSF predictions. This approach assumes some systematic biases are present in the reduced telemetry. The details of this approach are outlined in Fig. 5.

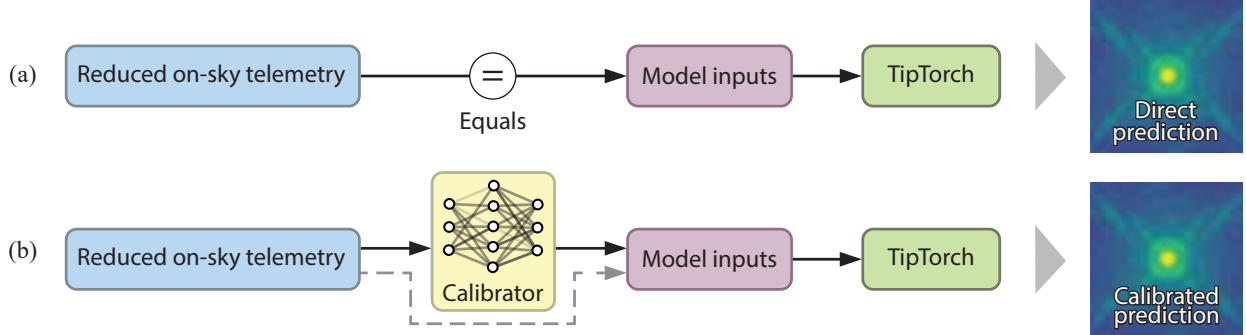


Figure 5. It has been demonstrated earlier that TipTop can accurately recreate on-sky PSFs provided correct inputs. However, the fitting showed that these inputs differ from the reduced telemetry. It was suggested, that a transformation (calibrator) can be found to map reduced telemetry to PSF model inputs, assuming a systematic relationship exists between the two. This calibrator is a feed-forward Neural Network (NN). Note, that some parameters are directly passed into the PSF model bypassing the calibrator as indicated in Tab. 1. This arrow will be later omitted.

We use a feed-forward Neural Network (NN) as a calibrator, which is trained to learn an implicit transformation from reduced telemetry to model inputs. The advantage of using an NN is its ability to efficiently handle non-linearities and learn latent correlations between input and output parameters from data. In this application, the network architecture can be very compact, which is beneficial since the datasets we use are very limited in number of samples. Then, the problem of determining the optimal calibrator reduces to the problem of training the NN. In this work, we proposed several approaches to this problem.

Table 1. A comprehensive yet non-exhaustive list of TipTorch inputs used to simulate SPHERE PSFs. Parameters that are "passed directly" are extracted from the reduced telemetry and directly used in TipTorch. Meanwhile, "calibrator inputs" are first passed to the calibrator to make it generate model inputs for TipTorch model.

Passed directly in TipTorch	Calibrator inputs	Model inputs
DM pitch, $N_{actuators}$	$r_0$	Flux normalization
Pupil/apodizer masks	Loop rate	WFS reconst. noise
Telescope pointing	Photons per [s] per WFS subap.	Tip/tilt jitter
$\lambda_{science}$ , $\lambda_{WFS}$	Wind speed (ground and 200 [mbar])	PSF background
$C_n^2$ profile	Wind dir. (ground and 200 [mbar])	
$L_0$		
Loop delay, loop gain		

It is also important to underscore that certain parameters essential for initializing the TipTop model are missing in the telemetry. In our particular case, the data related to tip/tilt jitter was not recorded in the reduced telemetry generated by the SPHERE instrument, and therefore, it had to be inferred by the calibrator based on other available inputs. Thus, the calibrator plays an indispensable role in the entire process.

### 4.1 Naïve approach to calibrator training

To train the calibrator NN, creating a training dataset that maps reduced telemetry to model inputs is crucial. To do it, the dataset of fitted model inputs is used. This approach assumes that systematic relations between the reduced telemetry and the fitting results are present in the training data. To generate the dataset of fitted parameters, the PSF model is sequentially fitted to each PSF in the on-sky dataset independently. The NN is then directly trained to learn the implicit transformation between reduced telemetry fitted parameters. Here and later in this work, we employ 300 H-band samples for training, while 60 samples are used for validation. The results of this approach are shown in Fig. 6ab.

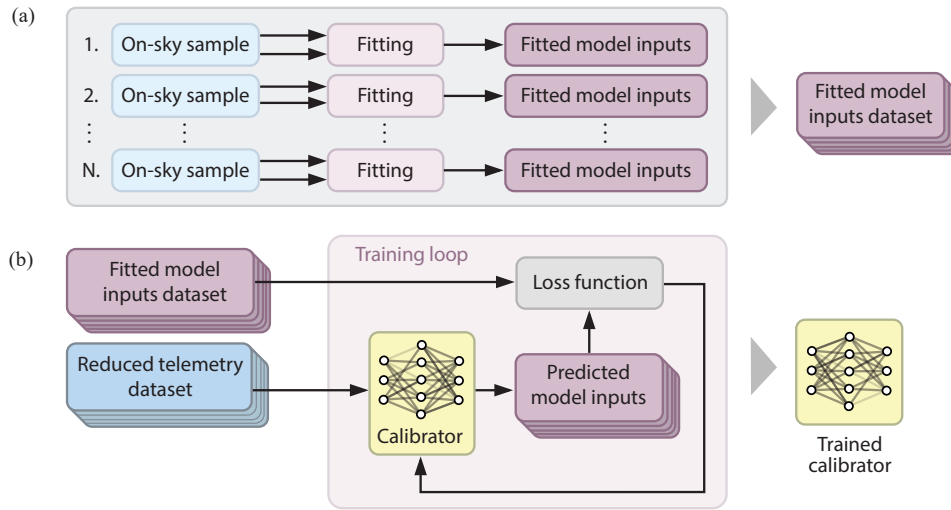


Figure 6. (a) The dataset of fitted PSF model parameters is created to train the calibrator. (b) The naïve approach for training the calibrator NN adopts the optimal model inputs that can be found via fitting and related to reduced telemetry via training the calibrator.

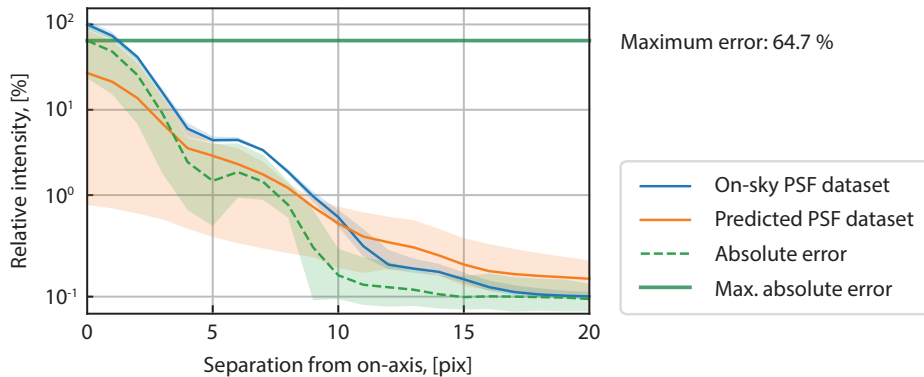


Figure 7. Radial profiles are predicted for the validation dataset. The prediction made by the calibrator, which was trained using a naïve approach, shows poor accuracy. The calibrator failed to generalize the transformation from the reduced telemetry to model inputs. This can mean that the correlation between them is absent. This can be attributed to overfitting, which resulted in creating an inconsistent dataset of fitted modal inputs.

One can see from Fig. 7 that this method leads to even inferior quality compared to previously discussed direct prediction when reduced telemetry was used without any preceding transformation applied. This can be caused by a weak correlation between initial estimations and fitting results, which can be attributed to *inconsistencies in the fitting outcomes*. During optimization, the model seeks parameter values that align with the morphology

of observed on-sky PSFs. However, it does not always maintain the physical plausibility of these values. The optimizer might settle into local minima instead of converging to a global one, overfitting to PSF morphology but yielding parameter values that are not physically meaningful.

One method to mitigate this is by incorporating regularization strategies like Maximum A Posteriori (MAP) probability. This approach minimizes not only the disparity between the generated and on-sky PSFs but also ensures that optimized parameters remain within physically meaningful ranges defined by their statistics. Nevertheless, this is only a partial remedy. MAP can yield biased estimates and does not guarantee convergence to the global minimum if the statistics of the regularized parameters are not precisely known.

The TIPTOP/TipTorch models are flexible, offering precise control over PSF morphology with multiple parameters (discussed in Sec. 1). However, these parameters can overlap in their effects on PSF morphology. For instance, the  $r_0$  parameter and tip/tilt jitter can influence the PSF morphology similarly, both manifesting themselves as a blur. Thus, the optimizer can identify multiple combinations of these parameters that achieve nearly identical training errors. Such scenarios represent ill-conditioned optimization problems where the landscape of the optimization criteria is notably flat, facilitating overfitting. One way to address this issue is by selecting the parameters with the most significant impact on PSF morphology, which reduces the size of the optimized parameters space. The present study focuses solely on fitting and predicting normalized flux, tip/tilt jitter, and WFS reconstruction noise. In our application to the SPHERE instrument, they are proven to impact PSF the most. The remaining model inputs are directly fetched from reduced telemetry bypassing the calibrator.

The issue of overparameterization is also directly connected to noise sensitivity. Models with too many parameters become particularly susceptible to training data noise. This hypersensitivity can lead to unpredictable optimization behaviors with minor data variations and a higher possibility of converging to local minima. This challenge is exacerbated by the low signal-to-noise ratio of some on-sky samples used for training. Moreover, extensive filtering of samples is not a practical solution, provided the limited size of our dataset.

In conclusion, all these factors described above make it challenging for the optimizer to converge a global minimum, making it more likely to converge into local minima instead. Consequently, individual sample fittings might be precise in terms of the accuracy of PSFs, but the overall fitted parameter distribution appears randomized across the dataset. Despite applying regularization and reducing the number of calibrated parameters to only a necessary subset, the results depicted in Fig. 7 remain unsatisfactory, with poor generalization capabilities. Ultimately, the solution to the problem lies in adeptly managing model complexity, necessitating a re-evaluation of our calibrator training strategy.

## 4.2 Joint training approach

We aim to introduce an alternative calibrator training method that demonstrates resilience against noise, reduces parameter coupling, and improves the generalization capabilities of the calibrator. The new proposed method integrates the PSF model directly inside the training loop of the calibrator, essentially implementing the physics-informed NN. Instead of linking reduced telemetry to the previously fitted model inputs, this approach directly bridges telemetry to corresponding PSFs via calibrator NN followed by the PSF model. The schematic representation of this technique is outlined in Fig. 8.

We perform training in a batch-wise manner. By doing so, the calibrator is trained to learn an implicit transformation that satisfies every sample in a given batch while all samples collectively contribute to the same loss function. Therefore, the optimizer simultaneously minimizes the error for all training samples, preventing any particular sample from dominating the loss. Additionally, since a single calibrator is shared for all training samples in the batch, the gradient updates collected from all data samples are averaged, increasing the robustness of the training loop to noise and mitigating the risk of overfitting. In Sec. 4.1, in contrast, the dataset of fitted model inputs was generated by fitting the model to each PSF individually, resulting in no cross-sample regularization. In this context, by loss function, we mean the Mean-Squared Error between the predicted and on-sky PSF cubes, and by sample, we mean the reduced telemetry with its associated on-sky PSF. The outcomes of this methodology are detailed in Fig. 9. The results reveal a significant improvement in accuracy. Although the error is still above 10%, the results are very promising.

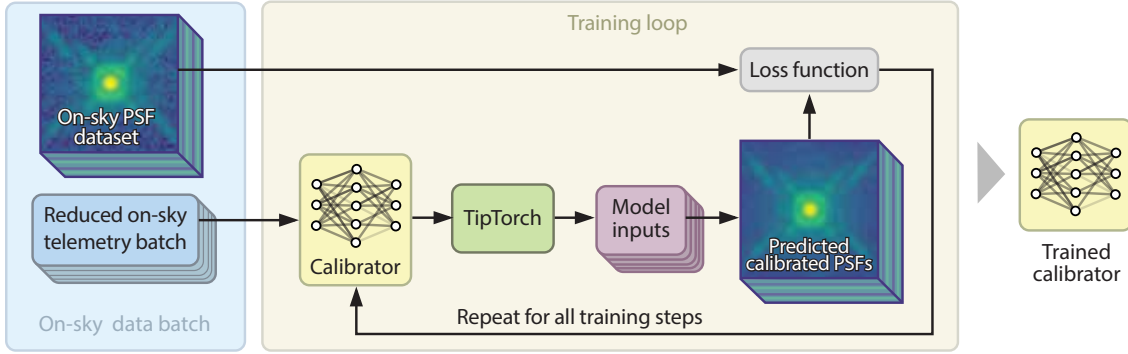


Figure 8. An alternate methodology for calibrator training integrates the PSF model directly into the calibrator training loop. Using this technique, the calibrator is trained to directly associate reduced telemetry with PSF morphology by backpropagating through the PSF model. The PSF model mitigates overfitting and incorporates underlying physics into the problem by acting as an implicit regularization.

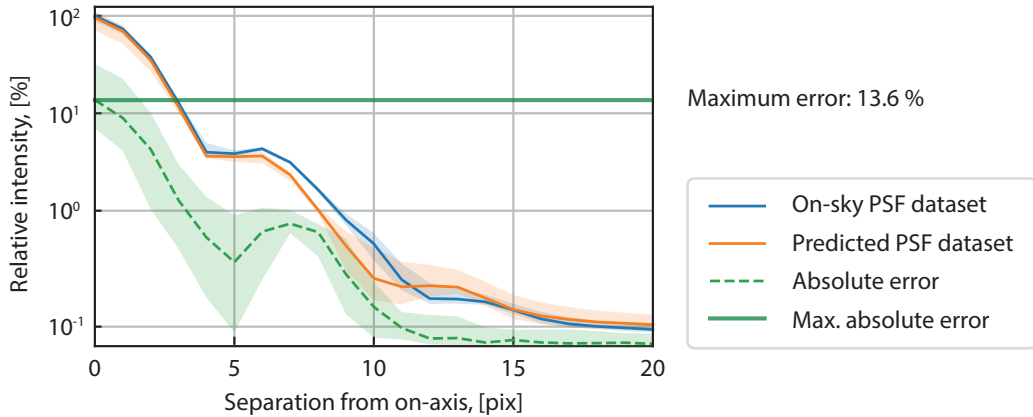


Figure 9. The proposed training approach significantly improves calibrator generalization capabilities, leading to improved accuracy when applied to real data. The profiles in this figure are computed for the validation dataset.

### 4.3 Training the calibrator on simulations

As discussed previously, on-sky data has its limitations. For example, realistic PSFs are prone to noise, while real telemetry can suffer from inaccuracies and measurement biases. Furthermore, the number of available on-sky samples is severely limited in our case. In fact, this problem is characteristic of most of the available on-sky datasets. This can be explained by the practical challenge of collecting a systematic, extensive PSF dataset simultaneously with associated telemetry and by the fact that the scientific community has generally given little attention to this issue before.

Therefore, it is crucial to eliminate the mentioned factors by testing the proposed techniques within a controllable environment to achieve clearer results. To do so, we ran realistic end-to-end simulations of SPHERE (IRDIS) using the OOPA0 code<sup>‡</sup>. In total, 10,000 H-band PSFs with associated telemetry were simulated. Unlike on-sky data, simulated telemetry is error-free, and PSFs are noiseless. The resulting synthetic telemetry underwent a reduction process analogous to on-sky telemetry. Initial parameters for simulations were sampled from real telemetry and site monitoring data.

Utilizing a comprehensive synthetic dataset allows us to re-evaluate the previously proposed techniques by

<sup>‡</sup><https://github.com/cheritier/OOPA0>

using simulated datasets and test the hypothesis that the accuracy of the considered approaches is indeed limited by the quality of datasets used and not by the PSF models.

First, the direct prediction is revisited. The methodology employed here is identical to the one introduced earlier in Sec. 2. One can see in Fig. 10a that, notwithstanding the complete controllable environment of OOPAO simulations, profiles directly predicted by TipTorch do not precisely match with OOPAO profiles (14.8% error). This discrepancy arises from the difference in the representation of specific input parameters between OOPAO and TipTorch, which introduces a bias in the telemetry, underscoring the necessity for using a calibrator.

Second, we revisited the procedure of calibrator training utilizing the fitted dataset. For this purpose, we fitted the TipTorch model to each synthetic PSF in the dataset and used the fitting results to train a calibrator that learns a relationship between the synthetic telemetry and the fitted model inputs. The method is identical to the one discussed earlier in Sec. 4.1, with the only difference being the utilization of simulated data.

As one can see, even though this approach earlier proved inaccurate with on-sky datasets (Fig. 7), the results shown in Fig. 10b demonstrate significantly higher prediction accuracy when synthetic data is used. In this case, the error of calibrated predictions reached down to 1.7% compared to the catastrophic 64.7% achieved earlier with on-sky data.

It can be explained by the fact that when the model inputs are fitted to noise-free PSFs, the optimizer is more prone to approach a true global minimum. This, in turn, facilitates the identification of more robust correlations between the reduced telemetry and the fitted optimal model inputs, facilitating the training of an accurate calibrator that can effectively rectify systematic biases in the input data and learn intricate relationships between the reduced telemetry and model inputs, resulting in enhanced prediction accuracy.

The subsequent steps involve assessing the influence of prediction precision on a synthetic dataset, considering varying amounts of photon noise and reduced telemetry errors. Additionally, exploring the training dataset size will be considered. Moreover, a joint training methodology incorporating synthetic data has yet to be attempted.

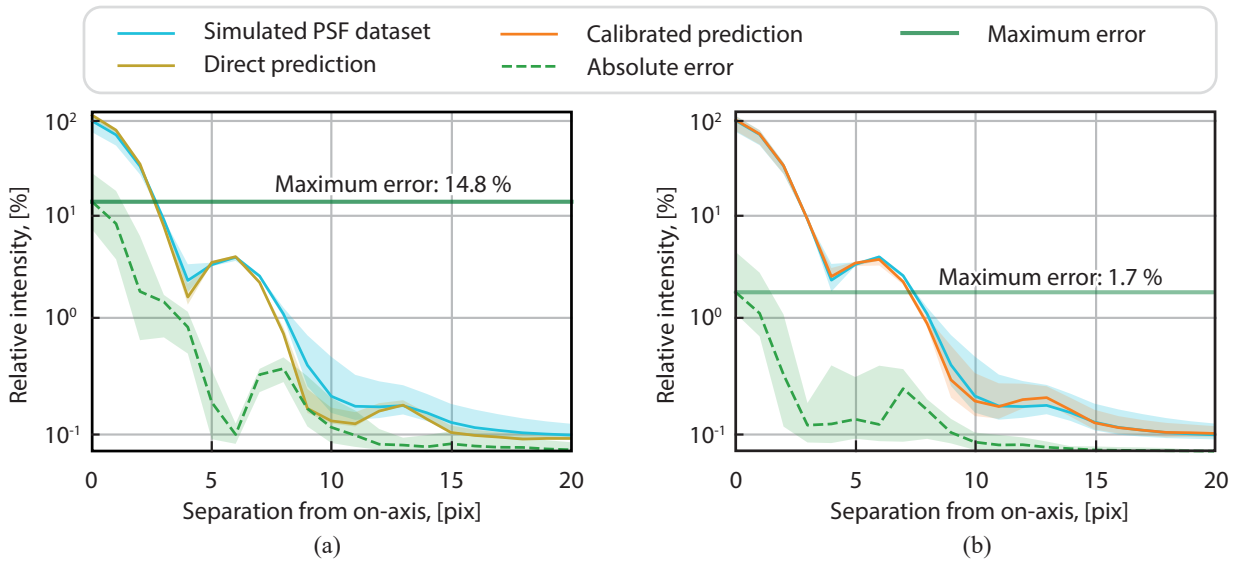


Figure 10. (a) Direct prediction using the synthetic reduced telemetry. Although simulations are fully controlled, the calibration is still required to match OOPAO and TipTorch models exactly. (b) The naïve approach to train calibrator was revisited for synthetic data. Despite very inaccurate prediction results obtained for on-sky samples earlier in Sec. 4.1, for synthetic samples, this approach resulted in a very high quality of prediction since clean, noiseless synthetic data were used for training the calibrator.

## 5. CONCLUSION AND FUTURE WORK

The observed results suggest that the prediction accuracy is mainly limited by the quality of the input data rather than by the PSF models. Model validation and experiments conducted using synthetic data have indicated that PSF models can yield highly accurate results when supplied with appropriate inputs. Therefore, the quality and quantity of available on-sky datasets might be the main concern within this scope. The lack of excessive and systematically recorded on-sky datasets limits the potential for developing accurate PSF predictors. While a few of these datasets are available, most remain poorly systematized and critically deficient in samples. Thus, it is crucial to log system telemetry associated with scientific PSFs in current and upcoming systems. It is worth mentioning that this data can be used not exclusively in PSF prediction but in various applications like system diagnostics and debugging.

As illustrated, fast and compact PSF models, like TipTop, can accurately model PSFs using a compact set of integrated parameters. This representation suffices for many PSF prediction tasks across varied instruments. This obviates the necessity of archiving complete telemetry consistently every night. Nevertheless, recording the full telemetry is sometimes still essential to create datasets that can be used in the future, e.g., to train the future generation of PSF predictors or, as was mentioned earlier, for system debugging and diagnostics.

To mitigate on-sky data scarcity, providing access to "digital twins" alongside scientific instruments is essential. This entails offering officially supported instrument simulation tools to the community. For example, for this research, we recreated the SPHERE IRDIS in OOPAO – a process that would have been unnecessary if pre-existing end-to-end simulations had been freely available. As shown, digital twins can be useful in compensating for the absence of on-sky data. They serve as valuable tools for instrument debugging in the design phase, as well as for research involving these instruments later. Additionally, digital twins can be utilized for pre-training machine learning models, as demonstrated in this study. The pre-trained models can then be fine-tuned with on-sky data. In this case, fine-tuning will require significantly fewer samples than training a network from scratch using only on-sky samples, which is practical in our applications when the number of on-sky samples is severely limited.

The forthcoming phase of this research involves developing a PSF-prediction framework for GALACSI NFM, leveraging the methodologies and techniques discussed in this work. After successfully implementing these techniques for NFM, this framework can be further extended towards ELT instruments.

## ACKNOWLEDGMENTS

We would like to express our profound gratitude to Vladimir Guzov, Olivier Beltramo-Martin, Julien Milli, Byron Engler, Cedric Taïssir Heritier, Marcos Suárez Valles, Pavel Shchekaturov, Joël Vernet, Jérôme Paufigue, and Guido Agapito. Their invaluable pieces of advice and profound expertise were pivotal in shaping and realizing this research. Their insights enriched the depth and rigor of our work. This work benefited from the support of the French National Research Agency (ANR) with WOLF (ANR-18-CE31-0018), APPLY (ANR-19-CE31-0011) and LabEx FOCUS (ANR-11-LABX-0013); the Programme Investissement Avenir F-CELT (ANR-21-ESRE-0008), the Action Spécifique Haute Résolution Angulaire (ASHRA) of CNRS/INSU co-funded by CNES, the ECOS-CONYCIT France-Chile cooperation (C20E02), the ORP-H2020 Framework Programme of the European Commission's (Grant number 101004719), STIC AmSud (21-STIC-09), the Région Sud and the french government under the France 2030 investment plan, as part of the Initiative d'Excellence d'Aix-Marseille Université -A\*MIDEX, program number AMX-22-RE-AB-151. This research has made use of computing facilities operated by the CeSAM data center at LAM, Marseille, France.

## References

- [1] Romain Fétick et al. "Physics-based model of the adaptive-optics corrected point-spread-function". In: *arXiv e-prints*, arXiv:1908.02200 (Aug. 2019), arXiv:1908.02200. DOI: [10.48550/arXiv.1908.02200](https://doi.org/10.48550/arXiv.1908.02200). arXiv: [1908.02200](https://arxiv.org/abs/1908.02200) [astro-ph.IM].
- [2] Benoit Neichel, Thierry Fusco, and Jean-Marc Conan. "Tomographic reconstruction for wide-field adaptive optics systems: Fourier domain analysis and fundamental limitations". In: *J. Opt. Soc. Am. A* 26.1 (Jan. 2009), pp. 219–235. DOI: [10.1364/JOSAA.26.000219](https://doi.org/10.1364/JOSAA.26.000219). URL: <https://opg.optica.org/josaa/abstract.cfm?URI=josaa-26-1-219>.

- [3] Benoit Neichel et al. “TIPTOP: a new tool to efficiently predict your favorite AO PSF”. In: *Adaptive Optics Systems VII*. Ed. by Laura Schreiber, Dirk Schmidt, and Elise Vernet. Vol. 11448. Society of Photo-Optical Instrumentation Engineers (SPIE) Conference Series. Dec. 2020, 114482T, 114482T. DOI: [10.1117/12.2561533](https://doi.org/10.1117/12.2561533). arXiv: [2101.06486](https://arxiv.org/abs/2101.06486) [[astro-ph.IM](#)].
- [4] Francois J. Rigaut, Jean-Pierre Veran, and Olivier Lai. “Analytical model for Shack-Hartmann-based adaptive optics systems”. In: *Adaptive Optical System Technologies*. Ed. by Domenico Bonaccini and Robert K. Tyson. Vol. 3353. International Society for Optics and Photonics. SPIE, 1998, pp. 1038–1048. DOI: [10.1117/12.321649](https://doi.org/10.1117/12.321649). URL: <https://doi.org/10.1117/12.321649>.
- [5] Jean-Pierre Véran et al. “Estimation of the adaptive optics long-exposure point-spread function using control loop data”. In: *J. Opt. Soc. Am. A* 14.11 (Nov. 1997), pp. 3057–3069. DOI: [10.1364/JOSAA.14.003057](https://doi.org/10.1364/JOSAA.14.003057). URL: <https://opg.optica.org/josaa/abstract.cfm?URI=josaa-14-11-3057>.